Physics informed data-driven near-wall modelling for lattice Boltzmann simulation of high Reynolds number turbulent flows

Citation for the original published paper (version of record):
Xue, X., Wang, S., Yao, H. et al (2024). Physics informed data-driven near-wall modelling for lattice Boltzmann simulation of high
Reynolds number turbulent flows. Communications Physics, 7(1).
http://dx.doi.org/10.1038/s42005-024-01832-1

(article starts on next page)

Colloids and Surfaces A: Physicochemical and Engineering Aspects 704 (2025) 135562

Contents lists available at ScienceDirect

Colloids and Surfaces A: Physicochemical and Engineering Aspects

journal homepage: www.elsevier.com/locate/colsurfa

Development of mesoporous silica-based active coatings for methylmercury removal: Towards enhanced active packaging

Przemysław Strachowski [a,*], Geeta Mandava [b], Johan Lundqvist [b], Romain Bordes [c], Mehdi Abdollahi [a]

[a] Department of Life Sciences – Food and Nutrition Science, Chalmers University of Technology, Gothenburg SE 412 96, Sweden
[b] Department of Biomedical Sciences and Veterinary Public Health – Swedish University of Agricultural Sciences, Uppsala SE 750 07, Sweden
[c] Department of Chemistry and Chemical Engineering – Applied Chemistry, Chalmers University of Technology, Gothenburg SE 412 96, Sweden

GRAPHICAL ABSTRACT

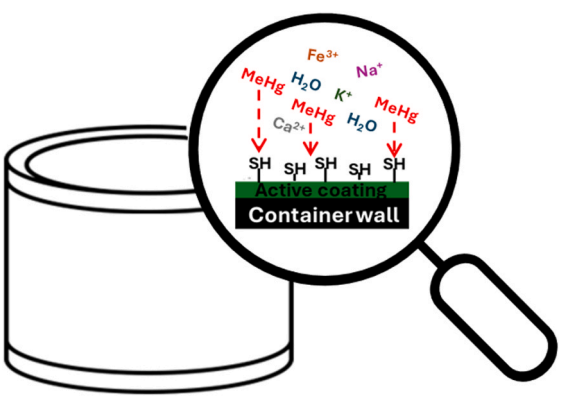

ARTICLE INFO

Keywords:
Adsorption
Active packaging
Food packaging
Coatings
Mercury

ABSTRACT

Active coatings capable of selectively removing pollutants are an innovative approach against human exposure to pollutants via food. This study aimed to develop an active coating capable of removing methylmercury from liquid food media. Thiolation of mesoporous silica particles modified via (3-Mercaptopropyl)trimethoxysilane increased their mercury adsorption capacity to 100 mg/g. The particles were successfully integrated into industrial, epoxy and polyurethane coatings but the induced mercury adsorption efficiency in the coatings was dependent on their type of binder. Scanning electron microscopy and energy-dispersive X-ray results revealed that the silica particles were entrapped within the coatings but remained more accessible to the external media in the industrial and polyurethane coatings. Thermogravimetric analysis confirmed the successful integration of the components. The kinetics of adsorption showed that the adsorption of methylmercury was achieved within a time range of 20-240 min, depending on the binder used in the coating. The methylmercury adsorption ability of the coatings was preserved in different food simulants and in the presence of competitive ions and in an

* Corresponding author.
E-mail address: pawelpr@chalmers.se (P. Strachowski).

https://doi.org/10.1016/j.colsurfa.2024.135562
Received 15 August 2024; Received in revised form 24 September 2024; Accepted 14 October 2024
Available online 15 October 2024

environment comprising cysteine. In vitro biosafety assays on different cell lines showed no negative effect from the silica modification on the safety of the coatings.

1. Introduction

Mercury, primarily in its methylated form has been identified as one of the most harmful neurotoxic pollutants present in aquatic food [1,2]. Although mercury is a naturally existing element, its elevated levels in the environment come from anthropogenic sources such as coal-fired power plants and mining. Inorganic mercury emitted by the industry is typically transported to the aquatic environment, converted to a more hazardous organic form, and subsequently accumulated by biota. Due to the bioaccumulative properties of methylmercury, fish and more generally seafood, have turned out to be the major source of exposure. The general observation is that the larger and older marine species, the higher their mercury contamination. For example, the average reported mercury concentration in the different tuna species originating from different parts of the world differs and is in the range 0.07–0.59 mg/kg [3–8]. Considering the anthropogenic emission of this pollutant and its environmental spreading [9,10], along with the relatively high consumption of seafood, mercury pollution of marine products has become a more and more concerning environmental issue. Among the efforts to limit chronic exposure of society to mercury via seafood, educational actions have been set forth including recommendations related to safety levels of fish consumption for various social groups (especially for children, pregnant and breast-feeding women), but also controlling and limiting the mercury emission [11–14]. Nevertheless, considering the significance of seafood as a valuable food source and the increasing focus on sustainable food production, there is a growing need for effective alternatives to preventive actions. Active food packaging could be a promising solution to address these concerns.

Compared to conventional packaging, active packaging is entirely or has some of its parts is involved in the post-production improvement of the packed food quality. This expands the function of packaging beyond its mechanical protection of the food, environmental shielding, or providing marketing information [15] to active interaction with the food to preserve the product quality. The technology is based on enriching the packaging or packaging materials with diverse additives or active agents that can actively deliver or remove some compounds to/from the packaging environment. Widely explored examples of active packaging include the gradual delivery of antimicrobial compounds to extend the product shelf-life by incorporation of essential oils [16,17], metal particles or nanoparticles [18–20] or antimicrobial peptides [21] into the packaging materials. Other examples of active food packaging are materials with the ability to remove oxygen or moisture via the incorporation of scavenging agents [22,23].

Some criteria must be fulfilled for the active agents when directly incorporated into the packaging materials. This is especially true for films to be industrially implementable. Firstly, the chosen agent must be safe enough from a food application perspective, then, the fusion of the packaging matrix (paper, polymers and biopolymers) and the active agent should be irreversible and chemically stable enough to avoid the uncontrolled release of any components into the packed product. Moreover, the addition of the active component should not negatively influence the mechanical and physical properties of the material, such as tensile strength or water resistance, etc. [24–26].

In this study, active coatings dedicated to capturing mercury from food mimicking aqueous media have been targeted as a novel approach for active food packaging. As mentioned earlier, the research on active food packaging over the past decade has been primarily focused on its ability to extend product shelf life. Notably, the great majority of published results are related to the development of various materials in the form of film which can be applied as a single or multicomponent package. The presented paper formulates a new approach for active packaging technology targeting the effective and selective removal of mercury from food products stored in a water medium. Furthermore, the research focuses on developing active coatings that can be applied to a wide range of currently used packaging materials (e.g., cans, jars). This technology offers a versatile coating solution, which is more beneficial than attempting to modify specific packaging materials. The authors hypothesized that there is a possibility of irreversibly immobilizing commonly used methylmercury adsorbents, such as thiolated silica, within a coating-forming matrix to create an adsorptively active coating. This novel approach facilitates the development of coatings capable of capturing mercury from aqueous environments, including liquid-based food products such as fish canned in water-based sauces. A more specific example would be minced fish canned in a water-based sauce, which creates a semi-fluid product. As mentioned earlier, fish products are recognized as one of the main sources of methylmercury in the human diet, however, other examples may include milk [27] or liquid rice-based products such as rice porridge or rice milk [28]. The container/can/jar can be coated with the developed lacquer which then plays its basic role of separating the food and packaging material and the new, additional role of a mercury scavenger.

The general concept of formulating active coatings for the adsorption of mercury is based on the hypothesis that the immobilization of thiol group carriers in a polymeric matrix can result in the creation of an affinity for mercury which is additionally promoted by the presence of an aqueous medium and the hydrophobicity of organic mercury [29]. In the present study, thiolated silica microparticles (chosen as economically justified material compared to silica nanoparticles) constituted the active ingredient. The efficient adsorption of mercury onto thiolated materials is a well-explored area in the literature so it is a natural starting point for the development of materials for the capture of mercury [30–34]. The choice of silica as a platform for hosting active adsorption sites in coatings, as an alternative to activated carbon, was motivated by its lack of impact on the color of the coating. Additionally, using silica microparticles for the production of such coatings provides an opportunity to utilize by-products from silica production (e.g., silica for chromatography). Literature reports the cases of mercury being released from fish tissues into the solution under the influence of -SH enriched external environment [35–37]. The main challenge for the synthesis of an efficient active coating for capturing mercury is to keep the active sites (thiol groups) accessible for the toxicant despite their partial entrapment and inactivation by the polymeric matrix. The hypothesis postulates that the use of spherical and/or semi-spherical mesoporous silica microparticles requires that they remain accessible to the fluid in the coating either via (i) their partial sticking out above the coating surface, (ii) prevention of complete blockage of their porous system by the polymer, or (iii) the generation of additional porosity in the coatings through the migration of silica particles during the polymer curing process, or a combination of thereof.

The study was aimed to develop a new generation of active coating by the development and incorporation of thiolated silica into different polymers (industrially in-use, epoxy and polyurethane) and prove the accessibility of the thiol groups in the coating for water-dissolved methylmercury. The efficiency of the active coating in the removal of methylmercury from aqueous media including food simulants and cysteine or mineral-containing competitive media was also investigated. A schematic overview of the study design is presented in Fig. 1.

2. Materials and methods

2.1. Chemicals

The mesoporous silica microparticles were obtained from Nouryon (Bohus, Sweden) and had particle size of 3–5 μm while having a specific surface area of 304 m^2/g. They were surface-modified with (3-Mercaptopropyl)trimethoxysilane (3-MPTMS, ≥95 %) as described below. Toluene and sodium hydroxide were purchased from Merck. Methylmercury (II) chloride standard water solution with a concentration 1000 mg/L (800 mg/L Hg) was purchased from Alfa Aesar®. Palladium (II) chloride (99.9 %) was supplied by Merck. A sample of an industrial, phenolic resin-based coating for light metal packaging (valPure™ 32S93MC) was provided by a fish processing plant. EpoFix Kit including epoxy resin and hardener was purchased from Struers. Castor oil (100 %) and Poly(hexamethylene diisocyanate, 99.5–100 %) for polyurethane resin preparation purchased from Merck. Standard solutions of Fe, K, Na, and Ca, ethyl alcohol, and acetic acid were purchased from Merc. 5,5′-Dithio-bis-(2-nitrobenzoic Acid) (Ellman's reagent or DTNB, ≥98 %), Glutathione, Potassium phosphate dibasic and Potassium phosphate monobasic were purchased from Merck. All dilutions and water solutions were prepared with ultrapure water freshly produced by Milli-Q® Advantage A10 Water Purification System (resistivity > 18 MW.cm).

2.2. Preparation of modified silica

The silica particles decorated with thiol groups were prepared by a two-step process including alkaline activation and subsequent thiolation of the pristine, calcinated material with a thiol alkoxysilane. Firstly, pristine silica was dried overnight at 105 °C and then the dry material was placed in a plastic 100 ml container with 0.5 M NaOH water solution with the silica mass/NaOH solution volume ratio of 1 g / 5 ml. The as-prepared mixture was shaken at 50 °C for 60 min using a water bath shaker. After the process was completed, the suspension was transferred to a centrifuge tube. The supernatant was removed, and the as-obtained powder was rinsed with water via five centrifugation and water change cycles. The activated silica was then dried overnight at 105 °C and subjected to a thiolation procedure. Dry silica (2 g) was placed in a round bottom flask containing 50 ml of toluene and then 1.89 ml of 3-MPTMS was added. The synthesis involved refluxing the suspension for 6 hours, followed by further purification of the powder with toluene through five cycles (centrifugation, removing the supernatant, and adding fresh toluene to the powder). Finally, the product (SiO_2-SH) was magnetically stirred with ethanol overnight to ensure that there were no residues of 3-MPTMS (which can be active in mercury binding). The modified silica was then dried overnight at the toluene boiling point (110 °C), and stored in a desiccator.

2.3. Active coating preparation

2.3.1. Industrial coating

The dry thiolated silica powder (SiO_2-SH) was vigorously mixed with the ready-to-use lacquer keeping 20 wt% of silica in the coating (considering 55 wt% dry mass content in the pure coating itself - based on our measurements). The highest possible homogeneity of silica distribution in the wet coating was guaranteed by using a mechanical homogenizer (IKA® T18 digital ULTRA TURRAXX) with 3200 rpm for 30 s. The dry active coating samples were prepared by using a film applicator, for this purpose 150 μm layer of the wet mixture was coated onto a stainless steel disc with a diameter of 40 mm and subjected to 30 min of hardening at 140 °C in a ventilated oven. The step-by-step preparation of the active coating is presented in Fig. S1.

2.3.2. Epoxy coating

The thiolated silica powder (SiO_2-SH) was mixed with a commercially available epoxy resin using a mechanical homogenizer (without the use of solvent). The silica content was kept at 20 wt%. After the mixture preparation, 13 wt% of the hardener was added and mixed manually for 15 min. The dry active coating samples were prepared by using the film applicator, for this purpose, 100 μm layer was coated onto a stainless-steel disc with a diameter of 40 mm and subjected to 24 hours of hardening at 30 °C.

2.3.3. Polyurethane coating

Castor oil-based polyurethane coating was prepared by mixing of castor oil and Poly(hexamethylene diisocyanate) with a mass ratio of 3:1. Then, 20 wt% of thiolated silica (SiO_2-SH) was added and the mixture was homogenized using a mechanical homogenizer. The dry active coating samples were prepared by using the film applicator, for this purpose, 100 μm layer was coated onto a stainless-steel disc with a diameter of 40 mm and subjected to 24 hours of hardening at 90 °C.

The term *modified coatings* refers to coatings altered through the addition of thiolated silica particles, enabling their activation for mercury adsorption.

2.4. Characterization of materials

2.4.1. Silica functionalization

Ellmans's method was applied to confirm the presence of thiol

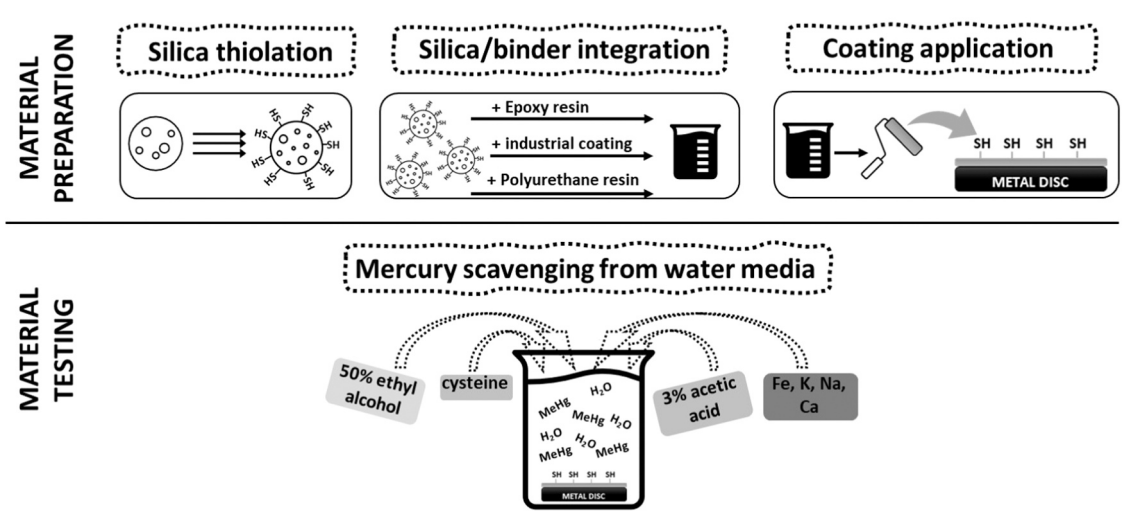

Fig. 1. Schematic overview of the study design.

groups in the modified silica powder. The theoretical basis of the method is described in detail elsewhere [38]. In brief, the method involves the reduction of 5,5′-Dithio-bis-(2-nitrobenzoic Acid) to the yellow-colored product by sulfhydryl (thiol) groups. The product can be easily quantified using a spectrophotometer based on its strong absorbance at 412 nm. Glutathione was used as a thiol group standard for the calibration curve. The series of standard solutions of glutathione were prepared by serial dilution of 1 mM stock solution of glutathione in phosphate buffer at pH=8. Each standard sample contained also Ellman's reagent at a concentration of 0.4 mg/ml. The samples were prepared by placing 10–15 mg of powdered thiolated silica in 30–100 ml of 0.4 mg/ml Ellman's reagent solution in phosphate buffer. The as-prepared suspensions were vigorously shaken for 20 min and then 250 μL of each solution was transferred to a 96-well plate and absorbance at 412 nm was measured using Tecan Safire 2 plate reader (Switzerland, Männedorf). Ellman's method is a well-known test for the quantitative determination of the sulfhydryl groups in liquid samples, thus the results obtained for silica powder were considered solely qualitative, yet they allow for a clear determination of the presence of thiol groups.

Surface area and porosity were analyzed by nitrogen sorption using a TriStar 3000 Surface Area and Porosimetry Analyzer (Low-temperature N_2 adsorption, Micromeritics, USA, Norcross) before and after functionalization. Thermogravimetric analysis (TGA/DSC 3^+ STAR® System, Mettler Toledo, USA, Columbus, N_2 atmosphere) of the pristine and modified material (active coatings enriched with thiolated silica) allowed to confirm the presence of additional chemical groups in the material structure after thiolation. Scanning electron microscopy (Zeiss Ultra 55 FEG, Germany, Jena, 4 nm gold sputtering by Leica EM ACE600) was used to investigate the morphological features of the silica powders.

2.4.2. Characterization of coatings

The presence of silica in the structure of the coatings was determined with EDX analysis (JEOL 7800F Prime, Japan, Tokyo). For the functionalized silica powder, Ellman's test (understood as a qualitative method) for the modified coatings was conducted. For this purpose, both sides coated metal disc was placed in the Petri dish containing 4 ml of Ellman's reagent followed by the same analytical procedure described above. Scanning electron microscope (SEM) imaging was also applied to investigate how the silica addition influenced the morphology of the hardened coating. The successful immobilization of modified silica within the structure of the coatings was confirmed by TGA under N_2 atmosphere. To collect the coating sample for this analysis, pieces of paint were carefully scraped off from the coated disc.

2.5. Study of the adsorption of methylmercury

2.5.1. Equilibrium adsorption study

Batch adsorption experiments were conducted to determine the adsorption isotherm of the modified silica. Around 15 mg of dry powder was placed in a vial containing 15 ml of methylmercury chloride standard water solutions with mercury concentration in the range between 20 and 160 mg/L. After 24 h of shaking, the suspension was centrifuged, and the supernatant was collected. Mercury concentration changes were determined using a flame atomic absorption spectroscopy (Agilent 200 series AA, USA, Santa Clara). The adsorption test for silica powder in a relatively high mercury concentration range was conducted in order to determine the full adsorption isotherm of this material, which revealed its adsorption potential as a raw component for coatings preparation.

The adsorption properties of the obtained coatings were tested via batch adsorption experiments conducted in duplicate. Blank tests without coatings addition showed that the losses of methylmercury resulting from adsorption on walls of the vials and other potentially uncontrolled processes were less than 5 %. The coated disc was placed in a Petri dish containing 7 ml of 0.3 mg/L methylmercury standard water solution (concentration calculated in relation to mercury) which represents the mercury concentration observed in the real canned fish samples. The coating surface to the volume of liquid ratio in the experiment was then ca. 3.5 cm^2/ml, whereas the ratio in the typical European tuna can with a diameter of 8.5 cm and height 3–4 cm containing 25–30 wt% of the sauce is ca. 4–5 cm^2/ml. The dish was then closed with a lid and sealed with insulating tape. The mercury concentration changes were determined after 24 h of sample incubation at room temperature by graphite furnace atomic absorption spectroscopy (GF-AAS, Agilent 200 series AA with GTA 120, USA, Santa Clara) using palladium (25 μg) as a chemical modifier of the furnace. Table S1 presents the heating program for the GF-AAS.

To simulate marine food conditions, competitive adsorption experiments were conducted. In this case, the coated disc was placed in a solution containing both 0.300 mg/L methylmercury and 0.365 mg/L cysteine which is responsible for the toxicant complexation in fish muscles. The cysteine concentration of 0.365 mg/L has been chosen to achieve a mercury/cysteine molar ratio of 1:2 to maintain an excess of cysteine in relation to mercury which guarantees its stabilization in the aqueous environment. The aim here was to create conditions unfavorable to the adsorption process.

Additionally, organic mercury adsorption tests from the solutions containing 3 % acetic and 50 % ethanol were conducted. The above solutions represent food conditions with hydrophilic and lipophilic properties, respectively and were designed based on the European Council Directive 85/572/ECC regarding tests for food-contact materials [39,40]. Competitive adsorption experiments from the minerals mixture were the next way to prove the applicability of the developing technology in the food industry. For that purpose, a mercury solution was enriched in Fe, K, Na and Ca with a concentration of 0.4 mg/L each. The objective of this series of experiments was to assess whether the presence of other minerals affects the adsorption performance of the coating in relation to mercury. Consequently, only the changes in mercury concentration were analyzed in this case.

2.5.2. Kinetic study

Adsorption rate parameters were evaluated with kinetic experiments, in which a sample of the coating in the form of coated metal discs was placed in a 7 ml water solution of methylmercury chloride with a mercury concentration of 0.3 mg/L. A 0.05 ml sample solution was collected after pre-defined time intervals between 1 and 240 min. In the case of adsorption kinetic for thiolated silica powder, the experiment was conducted according to the following procedure: A sample of 10 mg was placed in a series of identical methylmercury solutions (mercury concentration 0.3 mg/L). The samples were vigorously shaken for predefined duration (1–240 min) and then each sample was filtered to immediately terminate the adsorption process. The obtained samples of mercury solutions exposed to the active coating and silica powder at various times were analyzed with the GF-AAS. The results were presented as the relationship between the adsorption capacity (% of removed mercury) vs time.

2.6. Effect-based screening of materials

To evaluate the risk that the investigated materials could contaminate the food items with potentially health-hazardous compounds, an initial screening was performed with effect-based methods *in vitro*. Selected materials (described in 2.3.1. Industrial coating) were put into contact with water by placing 5 coated discs in a glass jar filled with 100 ml of MQ water. The prepared samples were sealed with Teflon tape, closed, and stored in darkness at room temperature for two weeks. The modified industrial coating, pure industrial coating, and uncoated disc were subjected to the tests. The water was then extracted using solid-phase extraction (SPE) and the extracts were evaluated for a number of human health-relevant toxicity endpoints. The extracts were tested at a relative enrichment factor of 1, taking into account both the

concentration over the SPE and the dilution in the cell culture media. A detailed methods description, including cell culture conditions, is presented in the Supporting Information. The applied *in vitro* assays are based on reporter gene technology, where the gene expression of a reporter protein is under the regulation of a DNA sequence that is responsive to the class of hazardous chemicals that are to be analyzed. Cell viability was monitored during all experiments, using the MTS assay, to ensure that analyses were conducted under non-cytotoxic conditions. The samples were analyzed for estrogenic, androgenic and anti-androgenic effects, oxidative stress and the potential to induce the aryl hydrocarbon receptor (AhR). A cell viability of >80 % of the control cells was regarded as non-cytotoxic.

3. Results and discussions

3.1. Characteristics of thiolated silica

Fig. S2 presents SEM images of the modified silica (SiO_2-SH). Table 1 shows the EDX analysis results which confirmed the presence of sulfur in the structure of the material. Modified silica particles occur mostly in the form of spherical particles with a diameter ca. 2 μm. Additionally, the presence of thiol groups was confirmed by Elmann's method and -SH surface concentration was found to be 0.27 ± 0.05 mmol/g. The specific surface area of silica was determined by nitrogen sorption and the obtained adsorption-desorption isotherms are shown in Fig. S3ab. The surface areas of pristine, activated and thiolated silica changed as follow: 304, 97 and 84 m^2/g which indicates collapsing and blocking of the porous structure under the basic condition of activation process and high-temperature conditions during thiolation. Moreover, the chemical groups introduced onto the surface occupy space in the pore network of the material. However, this was not reflected in the pore size distribution of the materials plotted in Fig. S3c. The pore size of the pristine material was in the range between 5 and 20 nm but the basic activation and thiolation process shifted the average pore size towards higher values in the range of 30–90 nm, as a result of the partial dissolution of the silica at high pH. Another way to confirm the presence of new groups on the surface was through TGA (Fig. 2). The mass changes in the temperature range up to 200 °C refer to the release of water absorbed by the material. 4–5 times more water in the activated and thiolated materials relates to the presence of a higher number of -OH, and -SH groups, thus enhancing the interaction of the material surface with water molecules. The curve for the thiolated material clearly reveals the presence of additional groups which were released at the temperature range 300–500 °C. Such a TGA curve profile is often observed for silica modified with SH groups [41–43].

3.2. Adsorption performance of modified silica

The adsorption isotherm of thiolated silica is presented in Fig. S4a; Fig. S4b, presents the adsorption behavior of the system in the low concentration range – below 1 mg/L. The maximum experimental adsorption capacity of mercury onto the thiolated silica was ca. 100 mg/g, which has been found as a relatively high in comparison to the other powdered material reported in the literature (Table 2). Table 2 shows additionally that the introduction of thiol groups into the material structure typically results in the most effective adsorbents. The shape of the adsorption isotherm found for our silica is typical for mercury adsorption [44,45], however, a deeper look at the isotherm in the range

Table 1
EDX results for the developed thiolated silica.

Element	Weight %	Atomic %
O	47.60 ± 0.51	61.57
Si	50.41 ± 0.50	37.14
S	1.99 ± 0.15	1.29

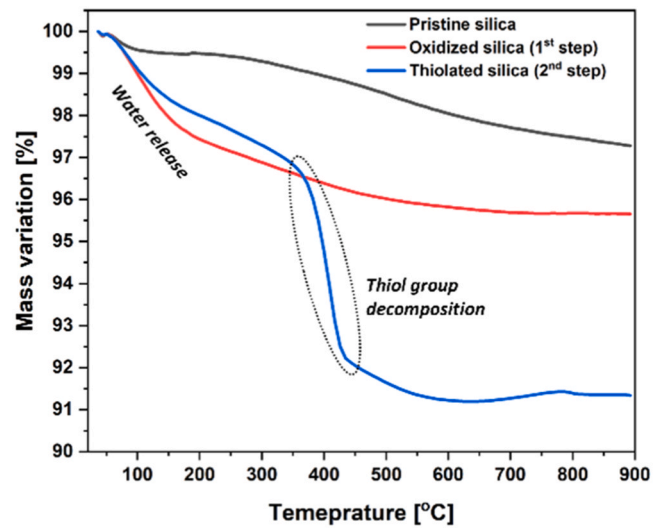

Fig. 2. TGA curves of pristine (black), NaOH activated (red) and thiolated silica (blue).

Table 2
The maximum adsorption capacity of methylmercury for different powdered materials.

Material description	Active site	Max. ads. cap. [mg/g]
Modified montmorillonite [49]	Thiol	39
Glutaraldehyde modified chitosan [50]	Nitrogen	0.0089
Barbital modified chitosan [50]	Nitrogen	0.0072
Graphene oxide/Fe-Mn composite [51]	Thiol	37
Modified magnetic mesoporous silica [45]	Thiol	14
Mechanochemically modified biochars [44]	Thiol	108
Modified graphene oxide [52]	Thiol	47

of low concentration reveals S-like shape which could indicate the partial input of the ion-exchange mechanism of mercury capturing [46]. The main mechanism considered in the case of mercury binding onto the thiolated materials is complexation (Hg-S bonds). However, the presence of hydroxyl cannot be excluded due to the material synthesis approach which involves basic activation of the pristine silica. The graph presenting the adsorption for relatively low-concentrated mercury revealed that the material is effective even in such a case (which is representative of the environmental samples). In other words, the material can effectively capture organic mercury even if its concentration in water is significantly below 1 mg/L which makes the as-modified silica promising as the active filler for the developing coatings. The Langmuir and Freundlich adsorption isotherm models [47,48] (equations in table S2) were applied to further quantify the considered process. R^2 coefficients describing the goodness of the model fitting to the experimental data are comparable and are equal to 0.939 and 0.946 for Freundlich and Langmuir, respectively. The calculation of the Langmuir isotherm parameters yielded a negative value of q_{max} which is not physically valid and can be related to the partial s-shape of the isotherm. Parameters K_F and 1/n for the Freundlich model were equal to 23.2 $(mg/g)(L/mg)^{1/n}$ and 0.967, respectively. The value of 1/n which has been found as very close to 1 represents the very high energetical homogeneity of the surface which is expectable in the case of the adsorption process based mainly on the interaction between the thiol groups immobilized in the silica structure and the mercury. Fig. S5 presents the single-point adsorption of methylmercury onto the silica in the subsequent stages of modification (the relatively high mercury concentration of 60 mg/L was chosen to determine sharp differences in the adsorption performance between different forms of silica used as a raw component) The curve clearly shows that the two-step modification including surface

activation and subsequent thiolation is the best method to obtain higher efficiency. Pristine silica is non-active in the process, activated-only and thiolated-only materials revealed very limited adsorption with a capacity of ca. 10 mg/g. Some adsorption performance for activated-only material was observed which confirmed the above-mentioned hypothesis of the ion-exchange mechanism. The reverse relationship between surface area and adsorption performance confirms that the adsorption effectivity depends on the presence of thiol group, not on the surface area itself.

3.3. Characterization of the coatings

Fig. 3 presents the TGA curves for the three unmodified and thiolated silica-modified coatings. In this analysis, the presence of silica-based additives is indicated by the increased mass of residues, which reflects the stability of silica under the analysis conditions. The differences between the mass residues for unmodified and modified coatings after the heat treatment of silica changed as follows: 20 % for the industrial, 11 % for the epoxy and 15 % for the polyurethane coating. The assumed silica content in each coating was equal to 20 % but the results reflected a lack of homogeneity of the distribution of the material in the polymeric matrix. Despite the expected differences in active particle distribution in the coating, TGA analysis confirmed the presence of silica, which was further supported by the results of EDX analysis. Additionally, the qualitative Ellman's method confirmed the presence of the thiol groups in the coating sample and their accessibility and absorption values were in the range covered by the calibration.

The morphology of the coatings is presented in Figs. 4–6. The microscopic surface architecture for all pure, hardened binders has been found as relatively smooth and simple, without visible porosity. Some micrometer-size objects can be noticed in the case of epoxy and polyurethane resins but this can rather be ascribed to the presence of impurities and dust particles attached to the wet surface during the longer hardening time of these resins in comparison to the industrial coating (24 h vs 30 min). The surface of the silica-modified industrial coating was rich in a few micrometers size spherical objects. Moreover, the EDX map confirmed that these objects consist of silica, oxygen and sulfur which clearly confirmed the presence of thiolated silica microparticles in the coating structure. A similar morphology was noted for the polyurethane-based material but in this case, the surface was less flat in comparison to the industrial coating and the surface concentration of the silica particles could be qualitatively evaluated as higher. The SEM images of the modified epoxy coating showed surface porosity and a significantly reduced surface concentration of silica particles in direct proximity to the surface. The presence of porosity in the epoxy resin structure could be attributed to the relatively long curing time and the low viscosity of the raw resin/hardener mixture which allowed the release of air bubbles. This could not be observed in the case of industrial coating due to the quick curing process and polyurethane resin which exhibited high viscosity. EDX analysis of the area occupied by the opening of the pores on the material surface has not revealed the presence of silica which indicated its possible presence in the lower layers of the coating. Nevertheless, some occurrence of silica on the surface of the material was also confirmed by the EDX measurements. In general, the analysis of the morphology of the synthesized materials revealed successful impregnation of the materials with silica particles. Their visibility directly at the surface suggests that they can play an active role in adsorption process. The cross-sectional SEM images of the coatings are presented in Fig. 7. It is clearly seen that for all pure coatings, the cross-sectional morphology is smoother in comparison to the modified ones and the way of fracture differs significantly between the unmodified and modified materials. In the case of silica-enriched industrial coating the filler particles are distributed in the whole volume, but the morphology of the material indicates a dense microscopic internal structure of the composite which is not observed for the epoxy coating. The epoxy-based active coating had a more open structure with visible discontinuities of the material. The cross-section views of the polyurethane material did not reveal the presence of silica in the material volume which is consistent with the observations for the top-view imaging showing the high surface concentration of the silica particles in the direct proximity of the coating surface.

The SEM and EDX analyses provided compelling evidence to support the hypothesis that the straightforward integration of silica nanoparticles into various coating structures leads to the partial entrapment of the filler. However, a portion of the silica remained accessible to the external environment in two possible ways – the occurrence of the particles at the material surface (industrial, polyurethane) and the creation of a porous structure in the material (epoxy).

3.4. Adsorption performance of the coatings

3.4.1. Methylmercury in water solution

Fig. 8 presents the results of the single-point removal of organic mercury from a water solution using pure and modified industrial, epoxy and polyurethane coatings. One of the expected observations is that the pure coatings which were rich in the chemical groups containing oxygen and nitrogen, were relatively active in mercury adsorption. It is also important to remember that methylmercury has a low solubility in water which generally promotes the adsorption onto hydrophobic sites. The pure industrial, epoxy and polyurethane coatings captured respectively 32, 34 and 67 % of mercury from the 0.3 mg/L water solution. Especially high adsorption performance of pure polyurethane resin can be ascribed to the presence of nitrogen which can interact with mercury [53]. The introduction of thiolated silica allowed for an increase in the adsorption effectivity to 88, 52 and 95 % for the industrial, epoxy and polyurethane active coatings, respectively. The experiments in the model system, under conditions that do not interfere with adsorption, allowed to conclude that the thiolated silica modification of the coatings

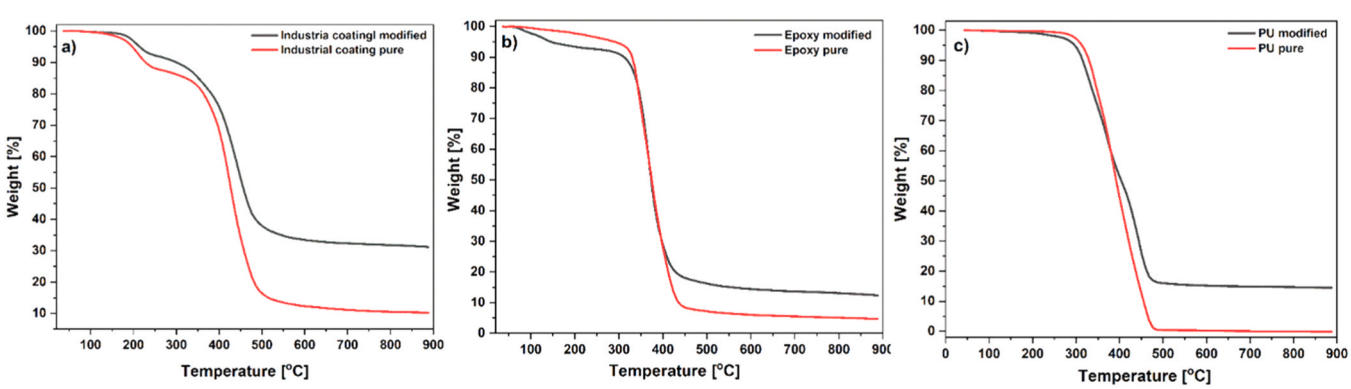

Fig. 3. TGA curves of pristine and modified coating based on (a) industrial coating; (b) epoxy resin and (c) polyurethane resin.

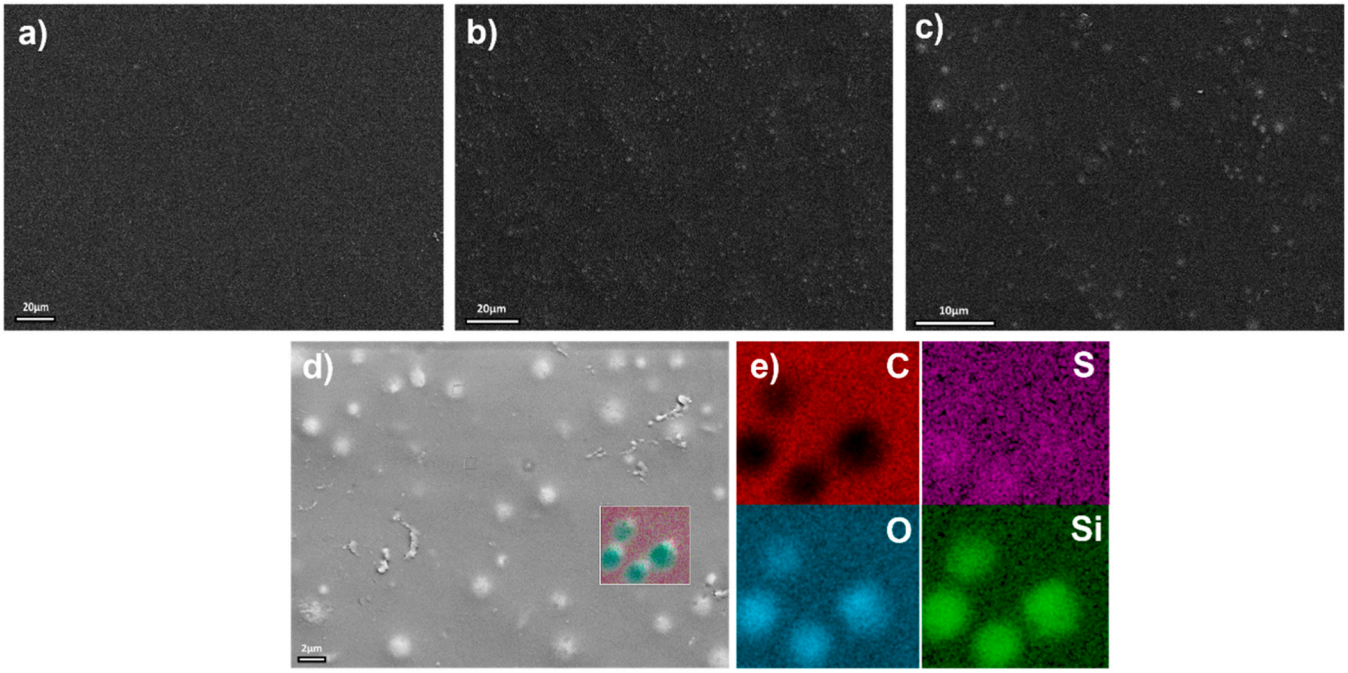

Fig. 4. SEM images and EDX maps of the industrial coating; (a) pure coating, (b-d) coating with SiO_2-SH (e) EDX of the industrial coating (C – carbon, S – Sulfur, O – oxygen. Si – silicon).

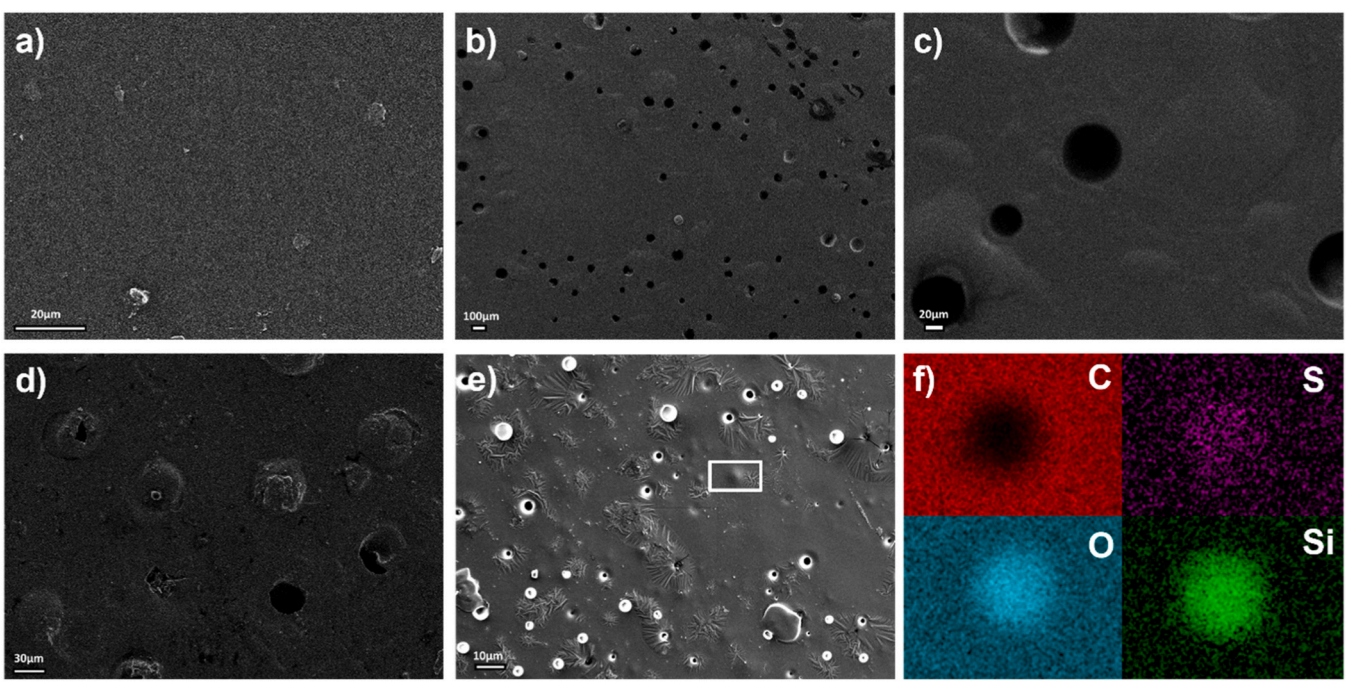

Fig. 5. SEM images and EDX maps of epoxy coatings; (a) pure coating, (b-e) coating with SiO_2-SH (f) EDX of the epoxy coating (C – carbon, S – Sulfur, O – oxygen. Si – silicon).

results in 42–175 % increase in the adsorption performance in comparison to the coatings alone.

3.4.2. Methylmercury in food-simulating media

The active coatings were developed with the intention of application in the food industry where the systems are significantly more complex and where interfering species are present. For this purpose, the methylmercury aqueous solution was enriched with cysteine at a concentration of 0.365 mg/L to simulate the mercury complexation with cysteine in fish muscles. This modification significantly increased the stability of mercury in the aqueous environment as seen in Fig. 8. The observed better performance of the active coatings in mercury removal compared to the pure coatings was seen here too. However, a noticeable decrease in the capture of the toxicant with all three activated coatings in the presence of cysteine was observed. The percentage of removed mercury from the solutions containing cysteine varied as follows: (i) pure and active industrial coating 25 % vs 34 %; (ii) pure and active epoxy coating 26 % vs 45 % and (iii) pure and active polyurethane

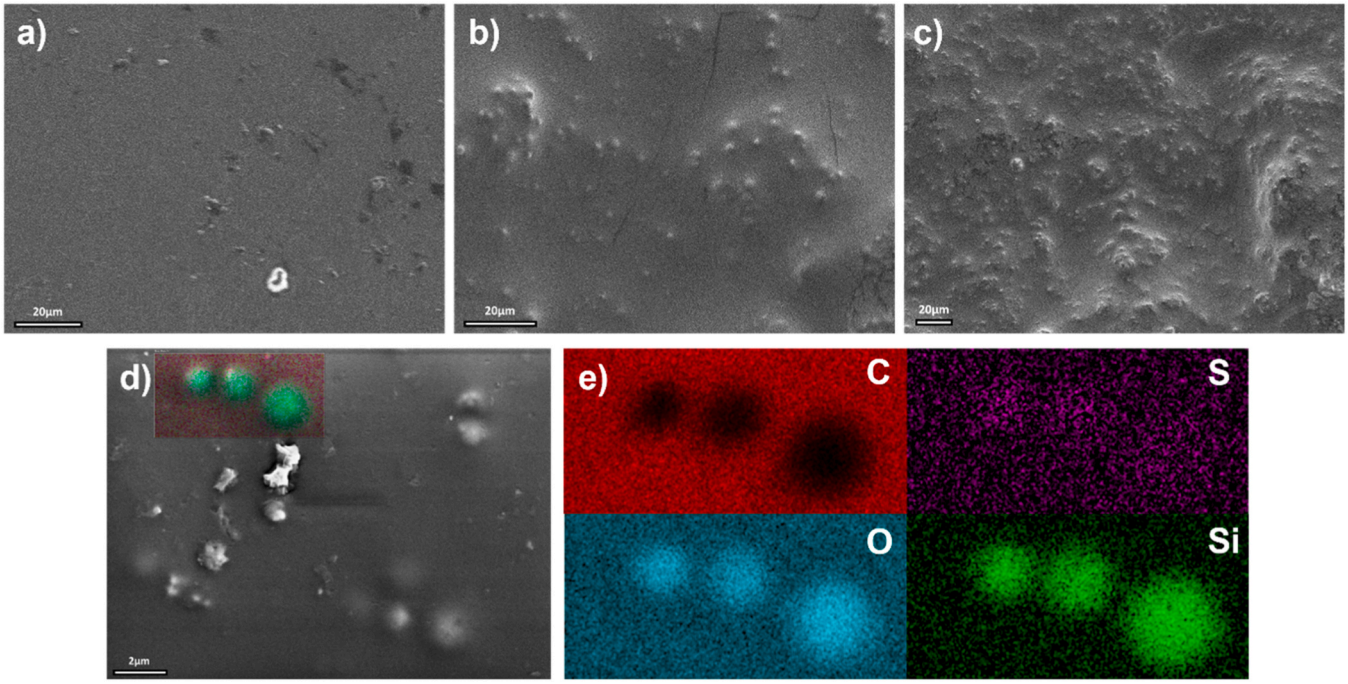

Fig. 6. SEM images and EDX maps of polyurethane coatings; (a) pure coating, (b-d) coating with SiO_2-SH, (e) EDX of the polyurethane coating (C – carbon, S – Sulfur, O – oxygen. Si – silicon).

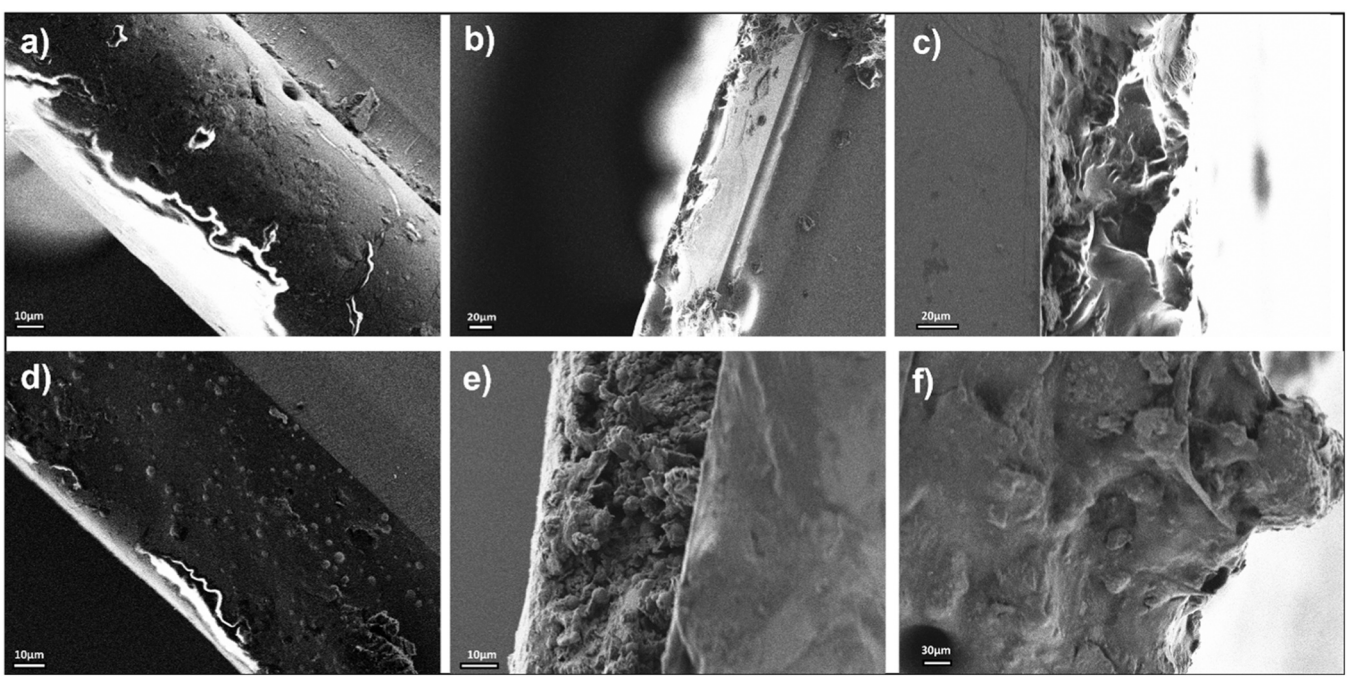

Fig. 7. Cross-sectional morphology of pure and modified coatings; (a) pure industrial, (d) industrial with SiO_2-SH, (b) pure epoxy, (e) epoxy with SiO_2-SH, (c) pure polyurethane, (f) polyurethane with SiO_2-SH.

coating 23 % vs 40 %. Modification of the industrial coating resulted in 36 % increase in the mercury adsorption, in the case of epoxy and polyurethane the increase was equal 73 %. Increasing the silica content up to 35 % in the coatings did not provide significant improvement.

Further tests simulating food conditions were conducted using the methylmercury aqueous solutions of ethyl alcohol and acetic acid at concentrations 50 % and 3 %, respectively (no cysteine added). Fig. 9a presents the results of mercury removal using the coatings from these food simulants solutions. One trial with the adsorption of methylmercury onto the modified industrial coating from 50 % ethanol/water solution containing cysteine was additionally conducted (Fig. 9a). The adsorption performance in 3 % acetic acid was limited to 50 % and 89 % of the performance respectively noted for industrial and polyurethane coatings in water. Noteworthy, the high mercury uptake by epoxy coating (93 %) in this condition was most probably caused by partial coating damage in acidic conditions, which resulted in releasing the silica into the solution. Applying 50 % ethanol as the mercury-containing medium resulted in a minor reduction of adsorption

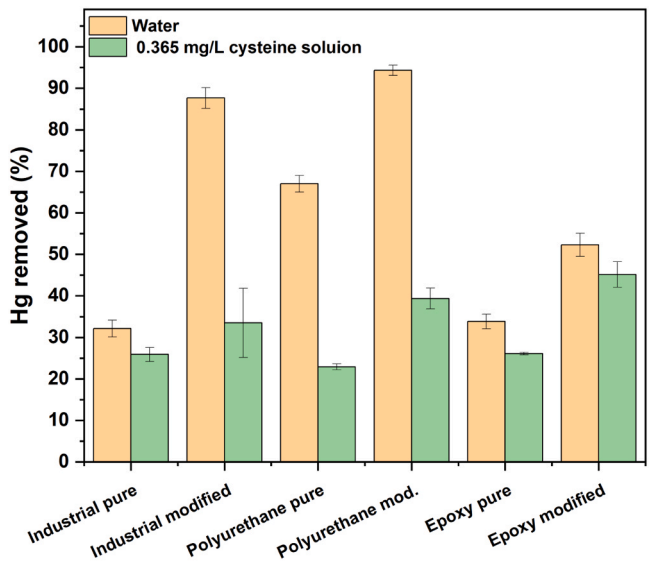

Fig. 8. Single-point adsorption of methylmercury (initial concentration 0.3 mg/L) onto the pure and modified coatings from water and cysteine/water solutions.

effectivity compared to pure water solution, which could be caused by higher methylmercury solubility in ethanol. The mercury removal effectivity in this case reached 78, 74 and 92 % of the performance observed in pure water solution for industrial, epoxy and polyurethane coating, respectively. In the case of 50 % ethanol-containing cysteine, no significant difference was observed, which indicated the usability of the developed technology in the case of complex solutions.

When considering the presence of heavy metal ions the occurrence of other metals should be considered, as Fe, Ca, Na, or K which may play a role as competitive adsorbing ions limiting mercury uptake by the coatings. To verify this, competitive adsorption experiments were conducted (Fig. 9b). Mercury removal was not affected by the presence of the other cations which commonly occur in food samples. This confirms that the functionalization of the coatings with thiol groups guarantees undisturbed mercury uptake even in the presence of other metal ions.

3.4.3. Kinetic of mercury uptake by the active coatings

The adsorption rate is often considered to have a crucial role in characterizing the effectiveness of the material employed in contaminants removal processes. In the context of canned product storage, the time required to complete the process has a secondary importance due to the relatively long predicted shelf life of such products. Nonetheless, the application of the developed technology can be expanded to broader domains, therefore the adsorption kinetics were determined. Fig. 10 presents the kinetic curves of mercury adsorption from the pure water and cystine-containing water onto the coatings containing or not thiolated silica particles. The kinetic curve for the powdered thiolated silica is not presented since the adsorption process onto this material has been found rapid and the maximum capacity was reached after less than 3 min. Adsorption using industrial coating was completed after 3.5–4 h independently of its modification and the presence of cysteine. Similarly, in the case of epoxy resin, the adsorption kinetics did not depend strongly on the material and solution composition, but the process was completed after 20–30 minutes. The time needed for the complete adsorption of mercury onto the polyurethane-based coating varied between 70 and 120 min.

The adsorption rate for different coatings changed as follows: industrial<polyurethane<epoxy and the difference between the coatings and powdered silica itself was very well-pronounced. This finding confirmed that silica is partially trapped in the polymeric structure of the coating binder which limits its availability for mercury. A direct comparison of the kinetic data and morphology revealed by SEM allows to conclude that the polymer layer of the industrial coating over the silica particles poses a stronger barrier for mercury than the porosity created by the modification of epoxy and polyurethane resins. The Weber-Morris intraparticle diffusion model allows for deeper insight into the adsorption kinetics. The model described in detail elsewhere [53,54], expressed by equation $q_t=K_D t^{0.5}+\Theta$ (look table S2) assumes that the overall adsorption kinetics can be limited by two main factors, namely, intraparticle diffusion described by coefficient K_D and barrier created by the fluid boundary layer on the material surface which can be quantitatively described by Θ (Θ represents the boundary layer thickness). The linearized kinetic curves are presented in Fig. S6, the multi-linear character of the results indicates multi-mechanisms of the adsorption kinetics control. However, the model coefficients outlined in Table 3 are calculated based on the first curve for each case, where both limiting factors play a significant role. The model was applied for

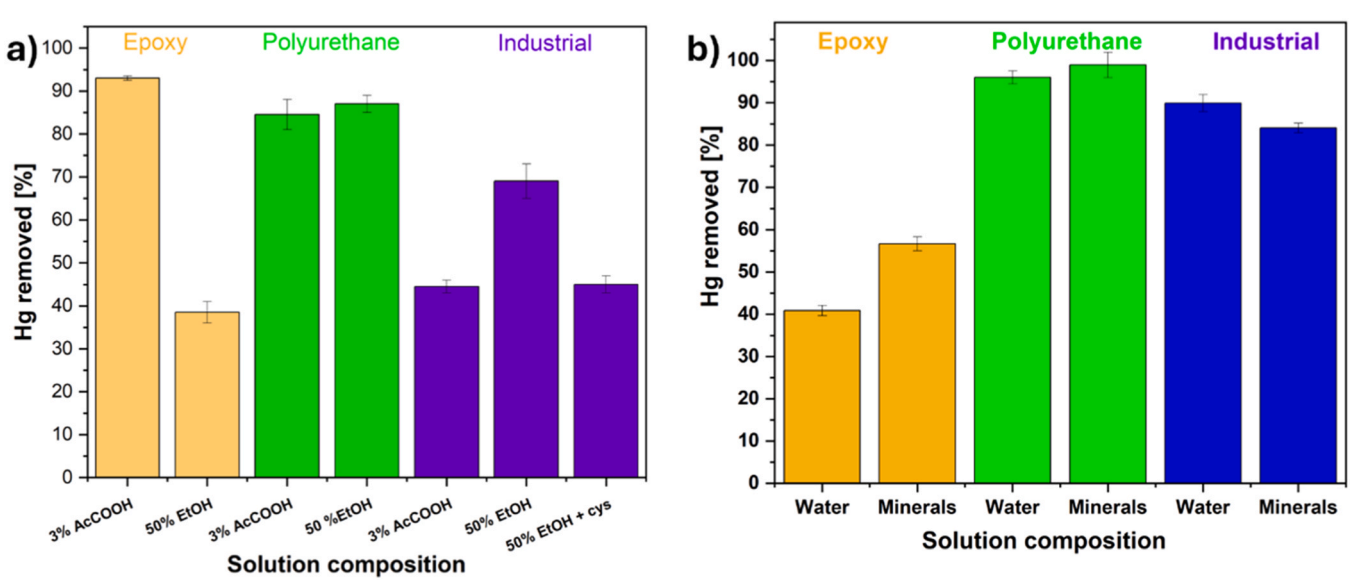

Fig. 9. Single-point adsorption of methylmercury (initial concentration 0.3 mg/L) onto (a) modified coatings from acetic acid, ethanol and cysteine solutions (3 % AcCOOH 3 % - acetic acid in water, 50 % EtOH – 50 % ethyl alcohol in water, 50 % EtOH + cys – 50 % ethyl alcohol in water + 0.365 mg/L cysteine) and (b) onto modified coatings from the mixture of Fe, Na, Ca and K ions at concentration 0.4 mg/L each.

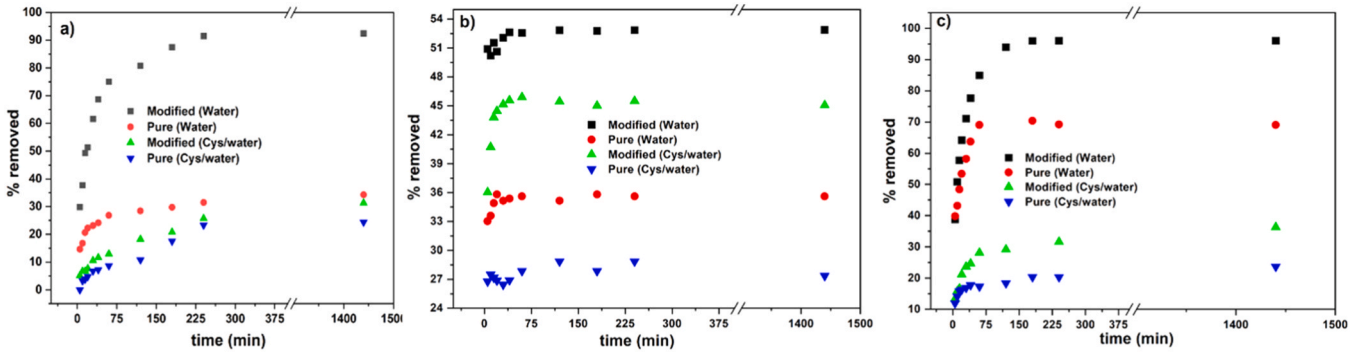

Fig. 10. Organic mercury adsorption kinetics curves onto the unmodified and modified coatings (a – industrial, b – epoxy, c – polyurethane).

Table 3
Intraparticle diffusion model coefficients for adsorption of mercury onto the industrial and polyurethane coatings.

Binder	System	K [mg g^{-1} $min^{-0.5}$]	Θ [mg/g]	R^2
Industrial	Pure – water	2.39	10.05	0.911
	Modified – water	9.57	8.97	0.986
	Pure – Cys/water	1.24	0.67	0.975
	Modified Cys/water	1.51	1.56	0.991
Polyurethane	Pure – water	6.03	25.44	0.990
	Modified – water	8.26	24.32	0.973
	Pure – Cys/water	1.35	9.75	0.901
	Modified Cys/water	2.79	8.24	0.967

industrial and polyurethane coatings due to significant adsorption delay in these cases; for epoxy resin-based coating the process was relatively quick and did not allow the use of this model. Regarding the values of Θ, one can notice that (i) Θ is always higher for the water solution in comparison with the cysteine-containing solutions and (ii) Θ is higher for the polyurethane coatings which indicates the presence of a thicker boundary layer on the polyurethane surface. This can be an indicator of quick adsorption of mercury onto the surface of the polyurethane matrix. The most important observation coming from the analysis of K_D coefficient is that their values were always higher for modified materials which indicated increasing input from intraparticle diffusion. This is an expectable behavior related to the introduction of porous silica into the coating structure which created additional barriers for the mercury transport from the solution to the active sites (mainly thiol groups) immobilized in the pore network of silica.

3.5. Effect-based evaluation of potential contamination by developed material

Water samples that had been exposed to unmodified industrial coating, modified coating, and uncoated metallic disc for two weeks were subjected to solid phase extraction and the extracts were then analyzed using *in vitro* bioassays to investigate if the materials had contaminated the water with any bioactive compounds. As a control, Milli-Q water was stored in the same type of container but without disk and coating. This water control was then concentrated and analyzed as described above.

The extract of water exposed to the modified coating showed estrogenic effects but on the same level as the extract of water exposed to unmodified coating, indicating that the modification does not increase the risk of contamination of estrogenic compounds (Fig. S7, panel A). Also the MilliQ control induced some estrogenic effects, but to a lesser extent. The extract of water exposed to the uncoated disk did not induce any estrogenic effects. Similar patterns of effects were observed for androgenic effects and oxidative stress (Fig. S7, panels B and C). No antiandrogenic effects were observed (data not shown). A clear AhR activity was observed both in extracts exposed to unmodified coating and in extracts exposed to modified coating (Fig. S7, panel D). The activity was higher in the industrial unmodified coating, indicating that the silica modification does not increase the risk of contamination of AhR inducing compounds. No cytotoxic effects were detected in either of the cell lines, at the applied exposure concentration.

4. Conclusion

This work reports the development of active coatings to be used in food containers such as jars or cans, with the function of removing mercury and improving food quality during storage time. Three coatings encompassing thiolated silica particles and based on (i) an industrially available coating for metal packages, (ii) epoxy, and (iii) polyurethane resins were developed. The presence of the thiol group plays a crucial role in binding mercury. Although the adsorption studies indicate partial trapping of silica in the polymer, which limits adsorption performance, the experiments demonstrated the promising activity and effectiveness of the coatings in reducing mercury levels under various conditions.

The coatings effectively captured 52–95 % of mercury from 0.3 mg/L aqueous solutions. The technology proved effective in reducing mercury concentration even in the presence of cysteine (34–45 % reduction), a mercury stabilizer and competitor. Additionally, the coatings remained effective in food simulant solutions such as acetic acid and ethanol. Their performance was not affected by the presence of iron, sodium, potassium, and calcium ions, which makes the material promising for application in real food systems. The methylmercury adsorption process using the active coatings was completed within 20–240 minutes, depending on the binder used.

Research on active coatings containing thiolated silica, dedicated to the removal of mercury from liquid phases containing food simulants and competing metal ions, paves the way for further development of this material concept. This may include more in-depth studies on the structure of the designed coatings, as well as additional application-oriented research, including the potential for material regeneration.

CRediT authorship contribution statement

Przemyslaw Pawel Strachowski: Writing – original draft, Visualization, Investigation, Conceptualization. **Geeta Mandava:** Investigation. **Mehdi Abdollahi:** Writing – review & editing, Supervision, Resources, Project administration, Funding acquisition, Conceptualization. **Johan Lundqvist:** Supervision, Methodology. **Romain Bordes:** Writing – review & editing, Funding acquisition, Conceptualization.

Funding

This work was supported by the Swedish Research Council- Formas (grant number 2020–00721).

Declaration of Competing Interest

The author is an Editorial Board Member/Editor-in-Chief/Associate Editor/Guest Editor for *Colloids and Surfaces A: Physicochemical and Engineering Aspects* and was not involved in the editorial review or the decision to publish this article. R. Bordes is Editorial Board Member and was not involved in the editorial review or the decision to publish this article

Acknowledgment

The authors would like to thank the Swedish Research Council - Formas for providing the grant to study within DetoxPak project (grant number: 2020-00721). We are also grateful to Olof Nyström from Packbridge AB for assistance in obtaining industrial coating samples.

Appendix A. Supporting information

Supplementary data associated with this article can be found in the online version at doi:10.1016/j.colsurfa.2024.135562.

Data availability

No data was used for the research described in the article.

References

[1] F.A.A. Goyanna, M.B. Fernandes, G.B. da Silva, L.D. de Lacerda, Mercury in oceanic upper trophic level sharks and bony fishes - a systematic review, Environ. Pollut. 318 (2023) 120821, https://doi.org/10.1016/J.ENVPOL.2022.120821.
[2] D. Cerveny, S. Roje, J. Turek, T. Randak, Fish fin-clips as a non-lethal approach for biomonitoring of mercury contamination in aquatic environments and human health risk assessment, Chemosphere 163 (2016) 290–295, https://doi.org/10.1016/J.CHEMOSPHERE.2016.08.045.
[3] C.V. Alva, E.T. Mársico, R. de O.R. Ribeiro, C. da S. Carneiro, J.S. Simões, M. da S. Ferreira, Concentrations and health risk assessment of total mercury in canned tuna marketed in Southest Brazil, J. Food Compos. Anal. 88 (2020) 103357, https://doi.org/10.1016/j.jfca.2019.103357.
[4] S. Mol, Levels of selected trace metals in canned tuna fish produced in Turkey, J. Food Compos. Anal. 24 (1) (2011) 66–69, https://doi.org/10.1016/j.jfca.2010.04.009.
[5] O. Miedico, C. Pompa, S. Moscatelli, A. Chiappinelli, L. Carosielli, A.E. Chiaravalle, Lead, cadmium and mercury in canned and unprocessed tuna: six-years monitoring survey, comparison with previous studies and recommended tolerable limits, J. Food Compos. Anal. 94 (2020) 103638, https://doi.org/10.1016/j.jfca.2020.103638.
[6] J. Burger, M. Gochfeld, Mercury in canned tuna: white versus light and temporal variation, Environ. Res. 96 (3) (2004) 239–249, https://doi.org/10.1016/j.envres.2003.12.001.
[7] F. Emami Khansari, M. Ghazi-Khansari, M. Abdollahi, Heavy metals content of canned tuna fish, Food Chem. 93 (2) (2005) 293–296, https://doi.org/10.1016/j.foodchem.2004.09.025.
[8] J. Ruelas-Inzunza, C. Patiño-Mejía, M. Soto-Jiménez, G. Barba-Quintero, M. Spanopoulos-Hernández, Total mercury in canned yellowfin tuna Thunnus albacares marketed in northwest Mexico, Food Chem. Toxicol. 49 (12) (2011) 3070–3073, https://doi.org/10.1016/j.fct.2011.07.030.
[9] J. Qi, et al., Primary suppliers driving atmospheric mercury emissions through global supply chains, One Earth 1 (2) (2019) 254–266, https://doi.org/10.1016/J.ONEEAR.2019.10.005.
[10] C.S. Yuan, C.E. Lee, I.R. Ie, K.C. Chiang, Y.L. Tseng, K.W. Wong, Seasonal variation and source identification of atmospheric speciated mercury in an industrial harbor area in East Asia, Sci. Total Environ. 815 (2022) 152785, https://doi.org/10.1016/J.SCITOTENV.2021.152785.
[11] A. Świerczok, M. Jędrusik, D. Łuszkiewicz, Reduction of mercury emissions from combustion processes using electrostatic precipitators, J. Electrostat. 104 (2020) 103421, https://doi.org/10.1016/J.ELSTAT.2020.103421.
[12] A.K. Karjalainen, et al., Estimated intake levels for Finnish children of methylmercury from fish, Food Chem. Toxicol. 54 (2013) 70–77, https://doi.org/10.1016/J.FCT.2012.02.074.
[13] J. García-Hernández, M.I. Ortega-Vélez, A.D. Contreras-Paniagua, D. Aguilera-Márquez, G. Leyva-García, J. Torre, Mercury concentrations in seafood and the associated risk in women with high fish consumption from coastal villages of Sonora, Mexico, Food Chem. Toxicol. 120 (2018) 367–377, https://doi.org/10.1016/J.FCT.2018.07.029.
[14] N.A. Connelly, T.B. Lauber, P.J. McCann, J. Niederdeppe, B.A. Knuth, Estimated exposure to mercury from fish consumption among women anglers of childbearing age in the Great Lakes region, Environ. Res. 171 (2019) 11–17, https://doi.org/10.1016/J.ENVRES.2019.01.005.
[15] K. Marsh, B. Bugusu, Food packaging - roles, materials, and environmental issues: Scientific status summary, J. Food Sci. 72 (3) (2007), https://doi.org/10.1111/J.1750-3841.2007.00301.X.
[16] S.A. Varghese, S. Siengchin, J. Parameswaranpillai, Essential oils as antimicrobial agents in biopolymer-based food packaging - a comprehensive review, Food Biosci. 38 (2020) 100785, https://doi.org/10.1016/J.FBIO.2020.100785.
[17] N. Vishnu Priya, U.G. Vinitha, M. Meenakshi Sundaram, Preparation of chitosan-based antimicrobial active food packaging film incorporated with Plectranthus amboinicus essential oil, Biocatal. Agric. Biotechnol. 34 (2021) 102021, https://doi.org/10.1016/J.BCAB.2021.102021.
[18] S. Bhople, et al., Myxobacteria-mediated synthesis of silver nanoparticles and their impregnation in wrapping paper used for enhancing shelf life of apples, IET Nanobiotechnol. 10 (6) (2015) 389–394, https://doi.org/10.1049/iet-nbt.2015.0111.
[19] A. Kalia, et al., Nettle-leaf extract derived ZnO/CuO nanoparticle-biopolymer-based antioxidant and antimicrobial nanocomposite packaging films and their impact on extending the post-harvest shelf life of guava fruit, Biomol 11 (2) (2021) 224, https://doi.org/10.3390/biom11020224.
[20] Y. Xing, et al., Antimicrobial nanoparticles incorporated in edible coatings and films for the preservation of fruits and vegetables, Mol 24 (9) (2019) 1695, https://doi.org/10.3390/molecules24091695.
[21] J.C.P. Santos, et al., Nisin and other antimicrobial peptides: Production, mechanisms of action, and application in active food packaging, Innov. Food Sci. Emerg. Technol. 48 (2018) 179–194, https://doi.org/10.1016/J.IFSET.2018.06.008.
[22] A. Dey, D.K. Sengupta, N. Raut, S. Neogi, Zero-valent metal incorporated cellulose acetate oxygen scavenging system for packaging of liquid food, Biocatal. Agric. Biotechnol. 50 (2023) 102735, https://doi.org/10.1016/J.BCAB.2023.102735.
[23] H.J. Escobar, J. Garavito, D.A. Castellanos, Development of an active packaging with an oxygen scavenger and moisture adsorbent for fresh lulo (Solanum quitoense), J. Food Eng. 349 (2023) 111484, https://doi.org/10.1016/J.JFOODENG.2023.111484.
[24] S. Priyanka, K.S. Raja Namasivayam, A.R. Bharani S, A. John, Biocompatible green technology principles for the fabrication of food packaging material with noteworthy mechanical and antimicrobial properties-a sustainable developmental goal towards the effective, safe food preservation strategy, Chemosphere 336 (2023) 139240, https://doi.org/10.1016/j.chemosphere.2023.139240.
[25] Y. Lei, L. Mao, J. Yao, H. Zhu, Improved mechanical, antibacterial and UV barrier properties of catechol-functionalized chitosan/polyvinyl alcohol biodegradable composites for active food packaging, Carbohydr. Polym. 264 (2021) 117997, https://doi.org/10.1016/J.CARBPOL.2021.117997.
[26] S. Bhowmik, D. Agyei, A. Ali, Bioactive chitosan and essential oils in sustainable active food packaging: recent trends, mechanisms, and applications, Food Packag Shelf Life 34 (2022) 100962, https://doi.org/10.1016/J.FPSL.2022.100962.
[27] Y. Wang, H. Qu, R. Wang, B. Dong, L. Zheng, Label-free biosensing of mercury(II) in milk using an aptamer-gated graphene field-effect transistor, J. Electroanal. Chem. 904 (2022) 115931, https://doi.org/10.1016/j.jelechem.2021.115931.
[28] X. Wang, Y. Wang, Y. Zhang, Z. Liu, X. Ji, Y. Cai, Mercury contents and potential exposure risk of rice-containing food products, J. Environ. Sci. 148 (2025) 683–690, https://doi.org/10.1016/j.jes.2024.02.004.
[29] P.K. Mehta, H. Park, E.T. Oh, H.J. Park, K.H. Lee, Tuning of distinguished fluorescent responses to methylmercury and Hg2+ ions: Selective detection of methylmercury over Hg2+ ions by fluorescent sensor using micelle system, Sens Actuators B Chem. 385 (2023) 133670, https://doi.org/10.1016/J.SNB.2023.133670.
[30] Y. Huang, Y. Gong, J. Tang, S. Xia, Effective removal of inorganic mercury and methylmercury from aqueous solution using novel thiol-functionalized graphene oxide/Fe-Mn composite, J. Hazard Mater. 366 (2019) 130–139, https://doi.org/10.1016/J.JHAZMAT.2018.11.074.
[31] L. Zhao, Y. Zhang, L. Wang, H. Lyu, S. Xia, J. Tang, Effective removal of Hg(II) and MeHg from aqueous environment by ball milling aided thiol-modification of biochars: effect of different pyrolysis temperatures, Chemosphere 294 (2022) 133820, https://doi.org/10.1016/J.CHEMOSPHERE.2022.133820.
[32] Y. Shen, et al., Thiol functionalization of short channel SBA-15 through a safe, mild and facile method and application for the removal of mercury (II), J. Environ. Chem. Eng. 6 (4) (2018) 5420–5433, https://doi.org/10.1016/J.JECE.2018.08.030.
[33] C. Lesaint, et al., Synthesis and characterization of mesoporous silicas functionalized by thiol groups, and application as sorbents for mercury (II), Stud. Surf. Sci. Catal. 156 (2005) 925–932, https://doi.org/10.1016/S0167-2991(05)80305-2.
[34] O. Hakami, Y. Zhang, C.J. Banks, Thiol-functionalised mesoporous silica-coated magnetite nanoparticles for high efficiency removal and recovery of Hg from water, Water Res. 46 (12) (2012) 3913–3922, https://doi.org/10.1016/J.WATRES.2012.04.032.
[35] I.C.M. Aizpurúa, A. Tenuta-Filho, A.M. Sakuma, O. Zenebon, Use of cysteine to remove mercury from shark muscle, Int J. Food Sci. Technol. 32 (4) (1997) 333–337, https://doi.org/10.1046/J.1365-2621.1997.00407.X.
[36] P. Hajeb, S. Jinap, Reduction of mercury from mackerel fillet using combined solution of cysteine, EDTA, and sodium chloride, J. Agric. Food Chem. 60 (2012) 6069–6076, https://doi.org/10.1021/jf300582j.
[37] P. Hajeb, J.J. Sloth, S. Shakibazadeh, N.A. Mahyudin, L. Afsah-Hejri, Toxic elements in food: occurrence, binding, and reduction approaches, Compr. Rev. Food Sci. Food Saf. 13 (4) (2014) 457–472, https://doi.org/10.1111/1541-4337.12068.

[38] G.L. Ellman, Tissue sulfhydryl Groups, Arch. Biochem. Biophys. 82 (1) (1959) 70–77, https://doi.org/10.1016/0003-9861(59)90090-6.
[39] EU food simulants. (1985) ⟨https://eur-lex.europa.eu/legal-content/EN/TXT/PDF/?uri=CELEX:31985L0572⟩, (Accessed 4 August, 2023).
[40] M. Lerch, R. Fengler, G.R. Mbog, K.H. Nguyen, K. Granby, Food simulants and real food – what do we know about the migration of PFAS from paper based food contact materials? Food Packag Shelf Life 35 (2023) 100992 https://doi.org/10.1016/J.FPSL.2022.100992.
[41] J. Meng, et al., Gold nanoparticles self-assemble on the thiol-functionalized fibrous silica microspheres to produce a robust catalyst, J. Phys. Chem. Solids 174 (2023) 111190, https://doi.org/10.1016/J.JPCS.2022.111190.
[42] S. Celine, S. Varun, A.M. Chandran, P.K.S. Mural, Electrospun PVDF/silica thiol nanofiber for chromium exclusion, Mater. Today Proc. 47 (2021) 1461–1465, https://doi.org/10.1016/J.MATPR.2021.03.689.
[43] S. Bagheri, M.M. Amini, M. Behbahani, G. Rabiee, Low cost thiol-functionalized mesoporous silica, KIT-6-SH, as a useful adsorbent for cadmium ions removal: a study on the adsorption isotherms and kinetics of KIT-6-SH, Microchem. J. 145 (2019) 460–469, https://doi.org/10.1016/J.MICROC.2018.11.006.
[44] L. Zhao, Y. Zhang, L. Wang, H. Lyu, S. Xia, J. Tang, Effective removal of Hg(II) and MeHg from aqueous environment by ball milling aided thiol-modification of biochars: effect of different pyrolysis temperatures, Chemosphere 294 (2022) 133820, https://doi.org/10.1016/j.chemosphere.2022.133820.
[45] G. Li, M. Liu, Z. Zhang, C. Geng, Z. Wu, X. Zhao, Extraction of methylmercury and ethylmercury from aqueous solution using surface sulfhydryl-functionalized magnetic mesoporous silica nanoparticles, J. Colloid Interface Sci. 424 (2014) 124–131, https://doi.org/10.1016/j.jcis.2014.03.026.
[46] V.J. Inglezakis, S.G. Poulopoulos, H. Kazemian, Insights into the S-shaped sorption isotherms and their dimensionless forms, Microporous Mesoporous Mater. 272 (2018) 166–176, https://doi.org/10.1016/j.micromeso.2018.06.026.
[47] B. Van der Bruggen, Freundlich Isotherm, in: E. Drioli, L. Giorno (Eds.), Encyclopedia of Membranes, Springer, Berlin, Heidelberg, 2014, https://doi.org/10.1007/978-3-642-40872-4_254-3.
[48] B. Irvinq Langmuir, Adsorption of gases on glass, mica and platinum. the adsorption of gases on plane surfaces of glass, mica and platinum, JACS 40 (9) (1918) 1291–1460, https://doi.org/10.1021/ja02242a004.
[49] P. Pei, Y. Xu, L. Wang, X. Liang, Y. Sun, Thiol-functionalized montmorillonite prepared by one-step mechanochemical grafting and its adsorption performance for mercury and methylmercury, Sci. Total Environ. 806 (2022) 150510, https://doi.org/10.1016/j.scitotenv.2021.150510.
[50] S. Kushwaha, P.P. Sudhakar, Adsorption of mercury(II), methyl mercury(II) and phenyl mercury(II) on chitosan cross-linked with a barbital derivative, Carbohydr. Polym. 86 (2) (2011) 1055–1062, https://doi.org/10.1016/j.carbpol.2011.06.028.
[51] Y. Huang, Y. Gong, J. Tang, S. Xia, Effective removal of inorganic mercury and methylmercury from aqueous solution using novel thiol-functionalized graphene oxide/Fe-Mn composite, J. Hazard Mater. 366 (2019) 130–139, https://doi.org/10.1016/j.jhazmat.2018.11.074.
[52] A.S. Krishna Kumar, S.J. Jiang, W.L. Tseng, Facile synthesis and characterization of thiol-functionalized graphene oxide as effective adsorbent for Hg(II), J. Environ. Chem. Eng. 4 (2) (2016) 2052–2065, https://doi.org/10.1016/j.jece.2016.03.034.
[53] G. Meyer, P. Nockemann, Affinity of divalent mercury towards nitrogen donor ligands, Z. Anorg. Allg. Chem. 629 (9) (2003) 1447–1461, https://doi.org/10.1002/zaac.200300161.
[54] W.J. Weber, A.M. Asce, J. Carrell, Kinetics of adsorption on carbon from solution, J. Sanit. Eng. Div. 89 (2) (1963) 31–59, https://doi.org/10.1061/JSEDAI.0000430.